ARTICLE

doi:10.1038/nature12863

Ferromagnetism in suspensions of magnetic platelets in liquid crystal

Alenka Mertelj[1], Darja Lisjak[1], Miha Drofenik[1,2] & Martin Čopič[1,3]

More than four decades ago, Brochard and de Gennes proposed that colloidal suspensions of ferromagnetic particles in nematic (directionally ordered) liquid crystals could form macroscopic ferromagnetic phases at room temperature. The experimental realization of these predicted phases has hitherto proved elusive, with such systems showing enhanced paramagnetism but no spontaneous magnetization in the absence of an external magnetic field. Here we show that nanometre-sized ferromagnetic platelets suspended in a nematic liquid crystal can order ferromagnetically on quenching from the isotropic phase. Cooling in the absence of a magnetic field produces a polydomain sample exhibiting the two opposing states of magnetization, oriented parallel to the direction of nematic ordering. Cooling in the presence of a magnetic field yields a monodomain sample; magnetization can be switched by domain wall movement on reversal of the applied magnetic field. The ferromagnetic properties of this dipolar fluid are due to the interplay of the nematic elastic interaction (which depends critically on the shape of the particles) and the magnetic dipolar interaction. This ferromagnetic phase responds to very small magnetic fields and may find use in magneto-optic devices.

A rich variety of complex self-assembled structures of colloidal particles in nematic liquid crystals that are the result of nematic-mediated anisotropic interaction between the particles is of wide-ranging interest for both fundamental science and applications[1–4]. Nematic liquid crystals are particularly interesting because of their coupling with external electric and magnetic fields. Ferromagnetic ordering in fluids has been experimentally observed in only two systems: liquid helium[5] and undercooled alloys at temperatures above 1,000 K (ref. 6). But more than 40 years ago, Brochard and de Gennes suggested that a true fluid ferromagnetic phase could appear at room temperature in a colloid of magnetic nanoparticles in nematic liquid crystal[7]. In such a system, orientational order of the nematic liquid crystal would impose orientational order on the anisotropic magnetic particles and, as in ferrofluids in an external magnetic field, magnetic ordering would also appear. Polar nematic ordering was first treated theoretically in ref. 8.

Ferrofluids are stable colloidal dispersions of monodomain magnetic nanoparticles in isotropic liquids, and are well known. Monodomain nanoparticles act as nanomagnets that begin to align in small magnetic fields. The magnetic interaction between the nanoparticles in ferrofluids is tuned so that in the absence of an external magnetic field, the average magnetic interaction of randomly oriented magnetic moments of particles at contact is smaller than thermal energy k_BT, so that the particles remain dispersed owing to entropic forces. When an external magnetic field is applied, magnetic moments on average orient along the external magnetic field. Because oriented magnetic dipoles attract head-to-tail, chaining of the particles along the external field occurs, leading to the well known increase of viscosity of a ferrofluid[9,10]. But whereas a ferrofluid becomes anisotropic only in an external field, the symmetry of the nematic phase of a liquid crystal is uniaxial. Nematic liquid crystals are composed of rod-shaped molecules that in the nematic phase on average orient along a common direction, called the director, that is usually denoted by a unit vector $\boldsymbol{n}$ with inversion symmetry $\boldsymbol{n} \equiv -\boldsymbol{n}$. The orientation direction can be controlled by external electric or magnetic fields or by preparation of confining surfaces, which can impose a defined orientation. Particles that are suspended in a liquid crystal and have a given orientation of $\boldsymbol{n}$ at the surface induce a deformation of orientation in the surrounding liquid crystal. This elastic distortion exerts a force on neighbouring particles at a range up to a few micrometres. In addition, defect lines or points can appear around particles. This liquid-crystal-mediated interaction can have either dipolar nature (when the defect is point-like) or quadrupolar nature (in the case of a line defect surrounding the particle) and can be either repulsive or attractive. Polydispersity, different shapes and/or different surfaces of the particles result in complicated structural forces between the particles, and only in simple cases have these been evaluated[11–13].

Magnetic nanoparticles in liquid crystal

A suspension of ferromagnetic nanoparticles in the isotropic phase of a liquid crystal behaves as any other ferrofluid. In the nematic phase, however, if the shape of the particles is anisotropic, they adopt a certain orientation with respect to the nematic order. For particles that are on average either prolate or oblate, nematic order has an effect similar to that of an external magnetic field, but with an important difference: because of the equality of the $\boldsymbol{n}$ and $-\boldsymbol{n}$ directions, the orientational ordering of the particles induced by the nematic phase is not enough for macroscopic magnetization to appear. For ferromagnetic ordering, a sufficiently strong magnetic interaction between the particles is necessary, but that causes aggregation, so a nematic-mediated repulsive interaction is needed. A single elongated particle, prepared so that the orientation of a nematic director $\boldsymbol{n}(\boldsymbol{r})$ (where $\boldsymbol{r}$ denotes the position vector in the medium) at its surface is parallel to the surface and to the particle's long axis, orients itself with its long axis parallel to $\boldsymbol{n}_0$ if placed in a nematic of average director orientation $\boldsymbol{n}_0$. The deformation of the nematic field is small and the resulting nematic interaction is too weak to prevent aggregation. Rod-shaped particles also tend to get next to each other, which leads to antiparallel magnetic dipoles. It has been shown[14] that, in a mixture of elongated ferrite particles in *N*-(4-methoxybenzylidene)-4-butylaniline (MBBA), magnetic hysteresis is obtained in a magnetic field of about 1 mT. The sample used in ref. 14, however, was spherical, with a diameter of 6 mm, the coercive

[1]J. Stefan Institute, SI-1000 Ljubljana, Slovenia. [2]Faculty of Chemistry and Chemical Engineering, University of Maribor, SI-2000 Maribor, Slovenia. [3]Faculty of Mathematics and Physics, University of Ljubljana, SI-1000 Ljubljana, Slovenia.

field depended on sample size, and no attempt was made to characterize either the orientation of the nematic or—in particular—the organization of the particles, that is, whether the particles were aggregated. In later experiments[15–19], aggregation was avoided by using only very diluted stable suspensions of elongated ferromagnetic particles in nematic liquid crystals, where the magnetic interaction between the particles was negligible and, consequently, in the absence of external magnetic field, macroscopic magnetization was not observed. The suspensions, however, showed paramagnetic behaviour, and in many cases the reorientation of the nematic director was observed at magnetic fields that were lower than the field needed to reorient pure liquid crystal.

If, on the other hand, the elongated particle is prepared so that the orientation of $\boldsymbol{n}(\boldsymbol{r})$ at its surface is normal to that surface, then it orients itself with its long axis normal to $\boldsymbol{n}_0$, and the particle's long axis can rotate in the plane perpendicular to $\boldsymbol{n}_0$. The nematic-mediated interaction is weakly attractive and such that the relative orientation between pairs of particles depends on their relative positions, again not stabilizing ferromagnetic order. In the first stable suspension of elongated particles treated for perpendicular surface orientation, the particles were oriented perpendicularly to the nematic director and the observed effects were independent of the direction of the external magnetic field[15]. The application of magnetic field along the director caused reversible flocculation of the particles, which was most likely to have been the result of field-induced distortion of nematic orientation that broke the rotational symmetry of the nematic phase and caused monopolar interaction between the particles[20].

Ferromagnetic order and magnetic domains

We show now that by using nanometre-sized ferromagnetic platelets with surface treatment that favours a perpendicular orientation of the nematic director at the particle surface, a stable nematic suspension can be produced with macroscopic spontaneous magnetization along the nematic director $\boldsymbol{n}_0$. This is the result of subtle interplay of the nematic-mediated force and the magnetic interaction between the particles. A platelet-shaped particle with planar surfaces treated such that $\boldsymbol{n}(\boldsymbol{r})$ at the surface is normal to the surface plane will orient itself with its surface normal parallel to $\boldsymbol{n}_0$. Pairs of such particles interact as quadrupoles (Fig. 1a). The quadrupolar nematic force between the particles gives the strongest attraction when the line joining two particles makes an angle of about 50° with respect to $\boldsymbol{n}_0$. At this angle, the interaction between two magnetic dipoles is small but still such that it favours parallel, that is ferromagnetic, ordering of the dipoles (Fig. 1a).

Preparation of a stable isotropic suspension of magnetic platelets is more demanding in comparison with spherical or elongated particles: this is due to large polydispersity and the fact that platelets form very stable aggregates because of their shape[21]. Recently, stable suspensions of scandium-doped barium hexaferrite single-crystal nanoplatelets in 1-butanol have been prepared with a narrower distribution of platelet size[22] (Fig. 1b), and we used these in our experiments. Barium hexaferrite has high magnetocrystalline anisotropy with a preferred direction of the magnetization along the *c* axis, which is perpendicular to the plane of the platelets. The thickness of the platelets is about 5 nm, and the distribution of the platelet diameter is approximately log-normal, with mean of 70 nm and standard deviation of 38 nm.

A suspension of magnetic platelets with number concentrations in the range 10^{13}–10^{14} cm^{-3} in liquid crystalline material pentylcyanobiphenyl (5CB) in the isotropic phase was used to fill planar glass cells; the interior surfaces of the cells imposed homogeneous orientation of the director in the plane of the sample. When the cells were slowly cooled, we observed many elongated aggregates forming at the nematic–isotropic phase boundary. This can be avoided by fast quenching into the nematic phase. Depending on platelet concentration, some sparse aggregates still remain (Extended Data Figs 1 and 2). Polarizing microscopy revealed that the nematic director in all samples is well aligned. The samples in the nematic phase are stable, and no additional aggregation occurs after several months and many exposures to external

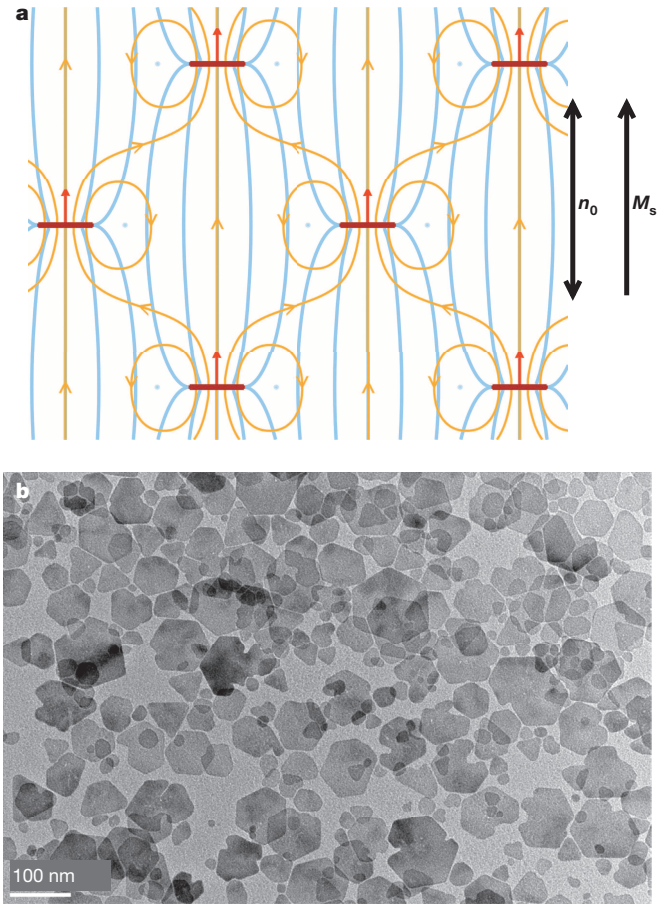

Figure 1 | Magnetic nanoplatelets. **a**, A schematic presentation of the distortion of the director (blue) and magnetic field (orange) around disk-like platelets (short, thick horizontal lines) represented side-on. Blue dots indicate cross-sections of disclination lines, and red arrows the directions of magnetic moments. The average director $\boldsymbol{n}_0$ and spontaneous magnetization $\boldsymbol{M}_s$ parallel to it are also shown. **b**, TEM image of magnetic platelets.

magnetic fields. When a small external magnetic field is applied, the aggregates in slowly cooled cells orient along the field direction while the surrounding nematic liquid crystal remains unchanged. The situation is completely different in quenched cells, where at a field of approximately 5–10 mT, growth of magnetic domains can be observed. Initially the domains are quite small, around 5 μm, then they grow up to a size of a few hundred micrometres (Extended Data Fig. 3). Further observations show that the response of the domains to an external magnetic field depends on the sign of the field, that is, the inversion symmetry of the nematic phase is broken, which is an indication of the spontaneous magnetization. Only two types of domains are observed. When the field is applied along the director, switching is observed only in one type of domain, while the other type of domain remains unchanged. If the direction of the field is reversed, the domains previously unchanged switch and those that switched before remain unchanged (Fig. 2b and c, Extended Data Fig. 1). If the field is applied in the direction perpendicular to the director, both types of domains switch and the domain walls are clearly visible (Fig. 2d and Extended Data Fig. 1). This behaviour shows that the spontaneous magnetization is along the director, and that the two types of domain have magnetization in opposite directions.

Magnetic hysteresis

Monodomain samples (confirmed to be single domain by polarizing microscopy; Extended Data Fig. 2) can be obtained by quenching the suspension from the isotropic to the nematic phase in an external magnetic field that is parallel to the nematic director. The magnetization

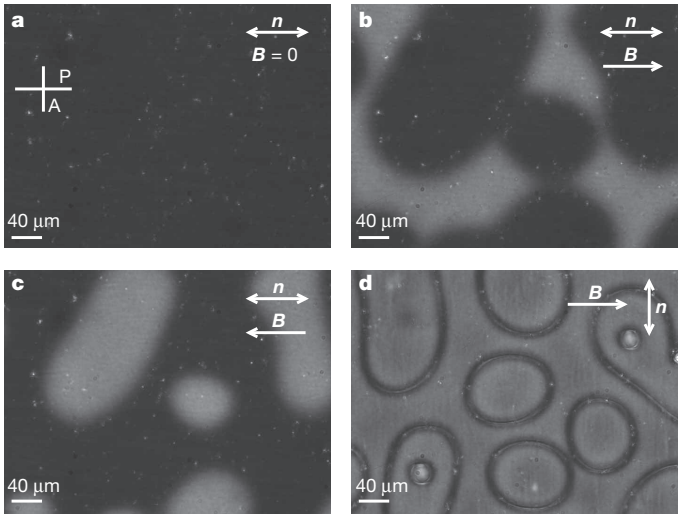

Figure 2 | Switching of ferromagnetic domains in an external magnetic field as seen by polarizing microscopy. The orientation of polarizer P and analyser A for all images is shown in **a**. **a**, Image of an ordered suspension of nanoplatelets in the absence of an external magnetic field ($\boldsymbol{B} = 0$). **b**, **c**, A magnetic field of 3.2 mT is applied along the director ($\boldsymbol{n}$) in opposite directions. **d**, A magnetic field of 16 mT is applied perpendicular to the nematic director. The dark lines are domain walls. Platelet concentration in 5CB is 0.16 wt%.

curves of such samples were measured using a vibrating-sample magnetometer (LakeShore 7400 Series VSM). From the magnetization curves we subtracted the diamagnetic contribution measured in a cell filled with pure 5CB, and obtained the magnetization curve belonging to the magnetic platelets (Fig. 3). In the absence of the external field, the magnetic moments of all platelets are oriented in the direction of the field used during sample preparation, and an external magnetic field applied in the same direction does not appreciably change the magnetization of the sample. When the field is applied in the opposite direction, magnetization along the director starts to decrease, reverses and then saturates. The absolute value of saturated magnetization is, within experimental error, the same as the magnetization at zero field, which means that all platelets have rotated by 180°. When the magnitude of the external field is slowly decreased, the magnetization returns to its initial zero-field value. A magnetic hysteresis is observed. At small concentrations the curves are shifted to negative values of H, whereas for a concentration of 0.3 wt% the curve becomes symmetric.

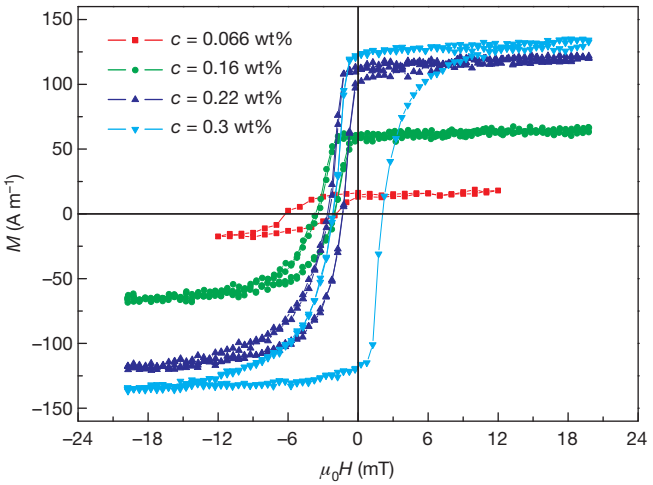

Figure 3 | Magnetization curves of monodomain samples show the switching behaviour of magnetic nanoplatelets in ordered nematic suspension. Magnetization curves are shown for four different platelet concentrations c (key at top left). At lower platelet concentrations, the magnetization in zero field returns to its initial value, whereas in the sample with concentration 0.3 wt%, the magnetization curve is centred around zero.

Observation of switching behaviour under a polarizing microscope (Extended Data Fig. 5) also shows that the nematic director is disturbed by the magnetic field. A field that is initially dark (the darkness showing that the optical axis, which is parallel to $\boldsymbol{n}$, is well defined) becomes brighter as the field is reversed, showing that in the field-reversed state $\boldsymbol{n}$ is distorted and cannot completely reverse owing to the orienting torques at the cell surfaces. At a higher concentration of magnetic platelets in a reversed field of about 10 mT, a system of two white lines crosses the optical field, switching it to the dark state (Fig. 4), that is, we get a complete reversal of the director. Pinning of the director at the cell surfaces causes the observed asymmetry of the hysteresis at lower concentrations. Such optical switching, occurring in a field that is antiparallel with the domain orientation, is unlike the usual Fredericks transition, which is a quadratic field effect in which the director field changes its orientation only when a field larger than a finite critical field is applied perpendicularly to $\boldsymbol{n}$. It also proves that coupling with the field is linear, as expected in a ferromagnet.

Shape matters

To explain the mechanism that prevents aggregation and produces spontaneous magnetization, we note the following. The structure of the nematic director field around a single disk-like platelet with strong perpendicular anchoring is of quadrupole symmetry with a defect line—that is, a disclination line (also called a Saturn ring) around the platelet (Fig. 1a). The exact structure of the nematic field depends on the size of the particle and the strength of the anchoring. The disclination line may not be present for very small platelet sizes, but in any case the leading interparticle interaction is quadrupolar. Recent molecular simulations showed that the Saturn ring can be present even around a spherical particle of the size of a few molecular lengths[23]. Experiments on colloidal suspensions of gold platelets of similar dimensions also show defects around the rim that are consistent with a Saturn disclination line[24]. Owing to the anchoring, the nanoplatelets in our system orient so that their plane is perpendicular to the nematic director $\boldsymbol{n}_0$, and, consequently, magnetic moments are parallel to $\boldsymbol{n}_0$. Magnetic interaction is mainly dipolar, favouring particles being vertically in register, while the nematic elastic interaction is quadrupolar, favouring an off-axis

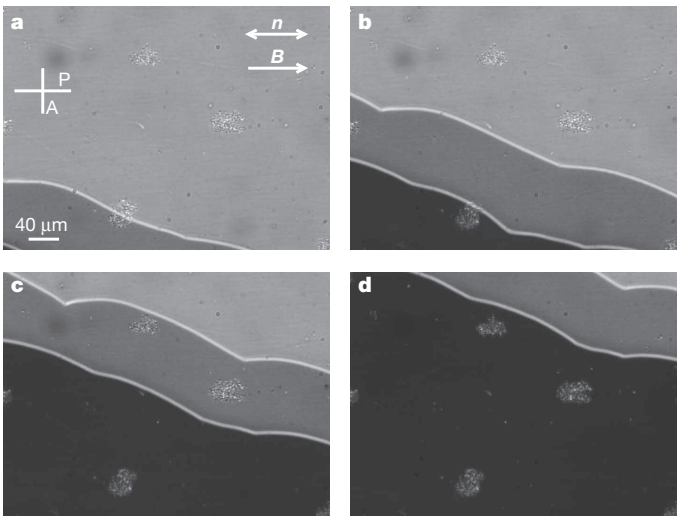

Figure 4 | Time sequence of images showing a complete switching of a monodomain sample. Time increases from **a** to **d**; time between images is 5 s. Images were obtained using polarizing microscopy; P and A in **a** show orientations of polarizer and analyser, respectively, for all panels; also for all panels, a field of 8.4 mT is applied parallel to $\boldsymbol{n}$ in the opposite direction to the magnetization. Travelling white lines are the surface domain walls, where the director rotates by π. The concentration of the platelets in 5CB is 0.3 wt%.

arrangement (Fig. 1a). The competition between forces reduces the total force to less than k_BT, but still induces ferromagnetic ordering by the magnetic interaction. This interplay of magnetic and elastic interactions works for plate-like particles and not for elongated ones. The platelets are also of different diameters, and polydispersity may also play a crucial role in the stability of the suspension, as has been shown in ferrofluids[25,26]. It has already been shown that molecules with oblate shape, with the dipoles along the short axis, enhance the degree of field-induced polarization in poled polymers[27].

Coupling of director and magnetization

Direct magnetic coupling of the nematic liquid crystal with the magnetic field is very weak, because the magnetic anisotropy of 5CB is very small, $\chi_a = 1.6 \times 10^{-6}$, where χ_a is the difference of magnetic susceptibility parallel to and perpendicular to $\boldsymbol{n}$. However, the direction of the magnetization is connected with the orientation of the platelets, which is (through surface interaction) coupled to the orientation of the director $\boldsymbol{n}$. In the Landau–de Gennes description, the free energy density f of a nematic liquid crystal in an external magnetic field that includes the lowest order of coupling between the director and magnetization can be written as[28,29]:

$$f = f_{nem} + \frac{\alpha}{2}M^2 + \frac{\beta}{4}M^4 - \mu_0 M\cdot H - \frac{1}{2}\gamma\mu_0(n\cdot M)^2 - \frac{1}{2}\chi_a\mu_0(n\cdot H)^2 \quad (1)$$

where the first term on the right hand side is the usual free energy density of nematic phase[28] f_{nem}, and the following three terms together give the magnetic free energy density: μ_0 is the vacuum permeability, and α and β are the Landau expansion coefficients describing the ferromagnetic transition. The last two terms describe the coupling of the nematic order with magnetization and external magnetic field, respectively. Whereas the direct coupling of $\boldsymbol{n}$ with the external field $\boldsymbol{H}$ is weak, its coupling with the magnetization $\boldsymbol{M}$ described by the constant γ can be much larger.

The behaviour of M with H, and the response to $\boldsymbol{H}$ under the polarizing microscope, can be explained by noting that the nematic director is locked in a given orientation by the orienting surface. So only the interior of the sample switches above a critical field while in a surface layer the director twists back to the initial orientation. The threshold field for the beginning of the reversal of M_s is $B_c = \pi^2\gamma\mu_0 K M_s/(K\pi^2 + \gamma\mu_0 M_s^2 d^2)$ (Methods, equation (5)), where d is the thickness of the sample, M_s the spontaneous magnetization and K the elastic constant associated with the distortion of $\boldsymbol{n}$; in our case, B_c is around 1 mT. This gives an estimate for γ of ~100. The orientation of $\boldsymbol{M}_s$ at the surface can switch either by breaking of surface anchoring (homogeneously) or by movement of surface domain π-walls (that can nucleate heterogeneously at sample edges or imperfections) in which the director turns by π. The critical field B_s needed to switch the surface orientation in the absence of nucleated π-walls can be estimated by noting that at B_s the magnetic coherence length $\sqrt{K/\gamma M_s B_s}$ must be of the order of the extrapolation length K/W, where W is the surface anchoring energy. This gives B_s around 100 mT for typical values of K and W, considerably more than what is observed, so that π-wall movement dominates (Fig. 4, Extended Data Figs 4 and 5). This also explains the observed hysteresis loops. For small concentrations, γM_s is too small to drive the movement of π-walls so surfaces mostly do not switch and the magnetization curves are shifted to negative H. For higher concentrations, γM_s is large enough that the surface can switch and the magnetization curve is symmetric. With π-wall movement a polydomain sample can be transformed to a monodomain one (Extended Data Fig. 4).

The system can be probed further by dynamic light scattering on orientational fluctuations in monodomain samples in external field. The well known turbidity of the nematic phase is caused by orientational fluctuations of the nematic director, which are the fundamental hydrodynamic excitations of director field $\boldsymbol{n}$. The relaxation rates of these excitations depend on the viscoelastic properties of the nematic liquid crystal and on external fields. Magnetization adds another degree of freedom coupled to $\boldsymbol{n}$, so that two types of fluctuations exist—one is more nematic-like and the other is more magnetic-like. Both are in principle observable by light scattering, but the nematic-like fluctuation is more pronounced. Whereas in the usual nematic phase the dependence of the relaxation rates on the external fields is quadratic, in the case of the presence of spontaneous magnetization M_s a linear term dominates, which is again an indication that the inversion symmetry of the nematic phase is broken. From the free energy density (equation (1)) we can calculate the relaxation rate of fluctuations in the magnetic field along the director (Methods, equation (4)). Experimental results are shown in Fig. 5. For small H, the relaxation rate depends linearly on the external field. At these magnitudes of magnetic field, the relaxation rate of pure 5CB does not change measurably. From values of spontaneous magnetization obtained from Fig. 3 and from the known K of 5CB, we can again estimate the coupling constant $\gamma \approx 50$–150, in accordance with the value obtained from magnetization curves.

Conclusion and outlook

We have demonstrated the existence of a ferromagnetic nematic colloidal suspension that was theoretically predicted long ago but not until now experimentally obtained. The system has the standard properties of a ferromagnet: monodomain samples can be prepared by cooling in an external field, and the system shows hysteretic behaviour, magnetization reversal in a flipped external field, and domain walls and domain-wall motion. It is an intriguing liquid that possesses two order parameters $\boldsymbol{n}$ and $\boldsymbol{M}$ and can therefore be considered a new class of multiferroic material. Ferromagnetic ordering is made possible by the shape of the magnetic nanoparticles that have the form of thin platelets. The quadrupolar nature of the nematic elasticity-mediated interaction prevents particle aggregation and causes the magnetic dipolar interaction to favour ferromagnetic ordering. The new phase switches at very small magnetic fields and may lead to new magneto-optic devices. Magnetization of the particles is a new degree of freedom that is coupled to the nematic order, which could lead to new effects—for example, oscillating director relaxation and field-dependent viscoelastic properties[30]. Incorporating the particles in other liquid crystal phases with chiral or smectic order would open up a new field of research, that of magnetic phenomena in complex fluids.

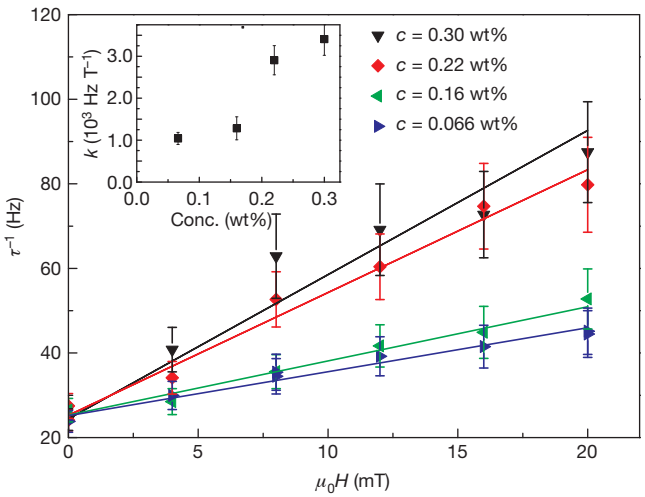

Figure 5 | Dependence of the relaxation rate of director orientational fluctuations on external magnetic field in samples with different concentration of magnetic nanoplatelets. Main panel, data for four different concentrations of platelets are shown (see key): τ^{-1}, relaxation rate. Inset, plot of k versus concentration of platelets (here k is the slope of τ^{-1} versus $\mu_0 H$). The given concentrations include all platelets, both well dispersed and aggregated, so the actual concentration of dispersed platelets is smaller than shown. Error bars, 1σ uncertainty of the least-squares fits.

METHODS SUMMARY

Barium hexaferrite nanoplatelets with the nominal composition $BaFe_{11.5}Sc_{0.5}O_{19}$ were hydrothermally synthesized at 240 °C (ref. 22). The nanoplatelets were dispersed in 1-butanol using dodecylbenzenesulphonic acid as a surfactant[21]. The thickness of the synthesized magnetic platelets is about 5 nm; the distribution of the platelets' diameter is approximately log-normal, with a mean of 70 nm and a standard deviation of 38 nm. Saturated mass magnetization of the platelets measured in the dried suspension was 32 A m^2 kg^{-1}, so the magnetic moment of an average platelet is 3×10^{-18} A m^2.

A suspension of 0.6 wt% magnetic platelets in 1-butanol was mixed with liquid crystalline material pentylcyanobiphenyl (5CB, Nematel) in the isotropic phase in different volume ratios. The mixture was kept in the isotropic phase at 50 °C for 24 h to evaporate 1-butanol. The final concentration of platelets in 5CB ranged from 0.06 wt% to 0.6 wt%. Suspensions, still in the isotropic phase, were used to fill planar glass cells, with surfaces imposing parallel orientation of the director (Instec, Inc.). The thickness of the cells was 20.4 μm. The cells were then quenched to give nematic phase. Quenching is necessary because in the samples that were slowly cooled into nematic phase, aggregation of platelets at the nematic–isotropic phase boundary appeared. In samples with a high concentration of platelets many aggregates were visible, however, the surrounding liquid crystal showed strong response to the external field (Extended Data Figs 1 and 2). The number and size of the aggregates decrease with decreasing concentration. At concentrations lower than about 0.06 wt%, the response of the sample to an external magnetic field is weak and inhomogeneous. The nematic–isotropic phase transition temperature of the suspensions is within experimental error (0.1 K) the same as for pure 5CB. Slow heating of the suspensions to give the isotropic phase again causes aggregation of the platelets at the nematic–isotropic boundary.

Online Content Any additional Methods, Extended Data display items and Source Data are available in the online version of the paper; references unique to these sections appear only in the online paper.

Received 19 June; accepted 8 November 2013.

1. Poulin, P., Stark, H., Lubensky, T. C. & Weitz, D. A. Novel colloidal interactions in anisotropic fluids. *Science* **275,** 1770–1773 (1997).
2. Muševič, I., Škarabot, M., Tkalec, U., Ravnik, M. & Žumer, S. Two-dimensional nematic colloidal crystals self-assembled by topological defects. *Science* **313,** 954–958 (2006).
3. Lapointe, C. P., Mason, T. G. & Smalyukh, I. I. Shape-controlled colloidal interactions in nematic liquid crystals. *Science* **326,** 1083–1086 (2009).
4. Lavrentovich, O. D. Liquid crystals, photonic crystals, metamaterials, and transformation optics. *Proc. Natl Acad. Sci. USA* **108,** 5143–5144 (2011).
5. Paulson, D. N. & Wheatley, J. C. Evidence for electronic ferromagnetism in superfluid ^{3}He-A. *Phys. Rev. Lett.* **40,** 557–561 (1978).
6. Albrecht, T. *et al.* First observation of ferromagnetism and ferromagnetic domains in a liquid metal. *Appl. Phys. A* **65,** 215–220 (1997).
7. Brochard, F. & de Gennes, P. G. Theory of magnetic suspensions in liquid crystals. *J. Phys.* **31,** 691–708 (1970).
8. Born, M. Über anisotrope Flüssigkeiten. Versuch einer Theorie der flüssigen Kristalle und des elektrischen Kerr-Effekts in Flüssigkeiten. *Sitz. Kön. Preuss. Akad. Wiss.* **30,** 614–650 (1916).
9. Ilg, P. & Odenbach, S. in *Colloidal Magnetic Fluids: Basics, Development and Application of Ferrofluids* (ed. Odenbach, S.) 249–326 (Springer, 2009).
10. Rosensweig, R. E. *Ferrohydrodynamics* 237–269 (Dover, 1997).
11. Senyuk, B. *et al.* Shape-dependent oriented trapping and scaffolding of plasmonic nanoparticles by topological defects for self-assembly of colloidal dimers in liquid crystals. *Nano Lett.* **12,** 955–963 (2012).
12. Senyuk, B. & Smalyukh, I. I. Elastic interactions between colloidal microspheres and elongated convex and concave nanoprisms in nematic liquid crystals. *Soft Matter* **8,** 8729–8734 (2012).
13. Eskandari, Z., Silvestre, N. M., Tasinkevych, M. & da Gama, M. M. T. Interactions of distinct quadrupolar nematic colloids. *Soft Matter* **8,** 10100–10106 (2012).
14. Rault, J., Cladis, P. E. & Burger, J. P. Ferronematics. *Phys. Lett. A* **32,** 199–200 (1970).
15. Chen, S.-H. & Amer, N. M. Observation of macroscopic collective behavior and new texture in magnetically doped liquid crystals. *Phys. Rev. Lett.* **51,** 2298–2301 (1983).
16. Kopčanský, P. *et al.* Structural changes in the 6CHBT liquid crystal doped with spherical, rodlike, and chainlike magnetic particles. *Phys. Rev. E* **78,** 011702 (2008).
17. Buluy, O. *et al.* Magnetic sensitivity of a dispersion of aggregated ferromagnetic carbon nanotubes in liquid crystals. *Soft Matter* **7,** 644–649 (2011).
18. Podoliak, N. *et al.* Macroscopic optical effects in low concentration ferronematics. *Soft Matter* **7,** 4742–4749 (2011).
19. Podoliak, N. *et al.* Magnetite nanorod thermotropic liquid crystal colloids: synthesis, optics and theory. *J. Colloid Interf. Sci.* **386,** 158–166 (2012).
20. Lev, B. I., Chernyshuk, S. B., Tomchuk, P. M. & Yokoyama, H. Symmetry breaking and interaction of colloidal particles in nematic liquid crystals. *Phys. Rev. E* **65,** 021709 (2002).
21. Ovtar, S., Lisjak, D. & Drofenik, M. Barium hexaferrite suspensions for electrophoretic deposition. *J. Colloid Interface Sci.* **337,** 456–463 (2009).
22. Lisjak, D. & Drofenik, M. Chemical substitution—an alternative strategy for controlling the particle size of barium ferrite. *Cryst. Growth Des.* **12,** 5174–5179 (2012).
23. Moreno-Razo, J. A. *et al.* Effects of anchoring strength on the diffusivity of nanoparticles in model liquid-crystalline fluids. *Soft Matter* **7,** 6828–6835 (2011).
24. Evans, J. S., Beier, C. N. & Smalyukh, I. I. Alignment of high-aspect ratio colloidal gold nanoplatelets in nematic liquid crystals. *J. Appl. Phys.* **110,** 033535 (2011).
25. Mahle, S., Ilg, P. & Liu, M. Hydrodynamic theory of polydisperse chain-forming ferrofluids. *Phys. Rev. E* **77,** 016305 (2008).
26. López-López, M. T., Zubarev, A. Y. & Bossis, G. Repulsive force between two attractive dipoles, mediated by nanoparticles inside a ferrofluid. *Soft Matter* **6,** 4346–4349 (2010).
27. Dalton, L. R., Harper, A. W. & Robinson, B. H. The role of London forces in defining noncentrosymmetric order of high dipole moment–high hyperpolarizability chromophores in electrically poled polymeric thin films. *Proc. Natl Acad. Sci. USA* **94,** 4842–4847 (1997).
28. de Gennes, P. G. & Prost, J. *The Physics of Liquid Crystals* 41–162 (Clarendon, 1995).
29. Pleiner, H., Jarkova, E., Muler, H. W. & Brand, H. R. Landau description of ferrofluid to ferronematic phase transition. *Magnetohydrodynamics* **37,** 254–260 (2001).
30. Jarkova, E., Pleiner, H., Müller, H.-W. & Brand, H. R. Macroscopic dynamics of ferronematics. *J. Chem. Phys.* **118,** 2422–2430 (2003).

Acknowledgements This work was supported by the Slovenian Research Agency (A.M. and M.Č., grant no. P1-0192; D.L. and M.D., grant no. P2-0089-4). We thank the CENN Nanocenter for use of the LakeShore 7400 Series vibrating-sample magnetometer.

Author Contributions A.M. designed the study and performed the experiments; A.M. and M.Č. interpreted results and wrote the paper; and D.L. and M.D. designed and synthesized nanoplatelets, and prepared the suspension of nanoplatelets in isotropic solvent.

Author Information Reprints and permissions information is available at www.nature.com/reprints. The authors declare no competing financial interests. Readers are welcome to comment on the online version of the paper. Correspondence and requests for materials should be addressed to A.M. (alenka.mertelj@ijs.si).

METHODS

Sample preparation. Barium hexaferrite nanoplatelets with the nominal composition $BaFe_{11.5}Sc_{0.5}O_{19}$, were hydrothermally synthesized at 240 °C (ref. 22). The nanoplatelets were dispersed in 1-butanol using dodecylbenzenesulphonic acid as a surfactant[21]. The thickness of the synthesized magnetic platelets is about 5 nm; the distribution of the platelets' diameter is approximately log-normal, with mean of 70 nm and standard deviation of 38 nm. Saturated mass magnetization of the platelets measured in the dried suspension was 32 A $m^2 kg^{-1}$, so the magnetic moment of an average platelet is 3×10^{-18} A m^2.

A suspension of 0.6 wt% magnetic platelets in 1-butanol was mixed with liquid crystalline material pentylcyanobiphenyl (5CB; Nematel) in the isotropic phase in different volume ratios. The mixture was kept in the isotropic phase at 50 °C for 24 h to evaporate 1-butanol. The final concentration of platelets in 5CB was from 0.06 wt% to 0.6 wt%. Suspensions, still in isotropic phase, were used to fill planar glass cells, with surfaces imposing parallel orientation of the director (Instec). The thickness of the cells was 20.4 μm. The cells were then quenched into the nematic phase. Quenching is necessary because in the samples that were slowly cooled into the nematic phase, aggregation of platelets at the nematic–isotropic phase boundary appeared. In the samples with high concentrations of platelets, many aggregates were visible, however, and the surrounding liquid crystal showed strong response to the external field (Extended Data Figs 1 and 2). The number and size of the aggregates decrease with decreasing concentration. At concentrations lower than about 0.06 wt%, the response of the sample to an external magnetic field is weak and inhomogeneous. The nematic–isotropic phase transition temperature of the suspensions is within experimental error (0.1 K) the same as for pure 5CB. Slow heating of the suspensions to the isotropic phase again causes aggregation of the platelets at the nematic–isotropic boundary.

Dynamic light scattering. We used a standard photon correlation set-up using a He-Ne laser with a wavelength of 632.8 nm, and an ALV-6010/160 correlator to obtain the autocorrelation functions of the scattered light intensity. The intensity of the laser beam was low and the measured correlation function did not depend on the intensity, so we conclude that no heating effects due to absorption were present in our measurements. The direction of the external magnetic field was along the director and in the same direction as the field used during the sample preparation, so that no reorientation of the director occurred when the magnitude of the field was increased. The director was in the scattering plane, and the wave vector of incoming light was perpendicular to the sample and the director. The scattered light was collected at a scattering angle of 2°. The polarizations of incoming and scattered light were horizontal, that is, both were extraordinary polarized, so that the splay-bend mode was measured[28]. The direction of gravity was in the plane of the sample perpendicular to the scattering vector. The scattering experiments were performed in samples with different concentration of platelets and in parts of the samples that were free of aggregates.

Polarizing microscopy. A Nikon Optihot 2-Pol microscope was used with an M Plan SLWD (20×) objective. Images were taken with a BW CCD camera (Pixelink PL-B957U) using PixeLINK Capture OEM software (Ver. 1.5.2.0). Gain was set to 0 and Gamma to 1.

Transmission electron microscopy. A drop of particle suspension in 1-butanol was deposited on a Cu grid and dried in air for transmission electron microscopy (TEM, Jeol, 2100). Images were taken with Gatan Digital Micrograph Software.

Relaxation rate of orientational fluctuations and critical field. Magnetization is a new degree of freedom that is coupled to the nematic director, so for each director mode in a normal nematic, there are two coupled modes in the ferromagnetic nematic. The relaxation rates of these modes can be calculated as follows.

The free energy density of a nematic liquid crystal in an external magnetic field that includes the lowest order of coupling between the director and magnetization can be written using equation (1) from the main text, which we reproduce here[28,29]:

$$f = f_{\mathrm{nem}} + \frac{\alpha}{2}M^2 + \frac{\beta}{4}M^4 - \mu_0 M\cdot H - \frac{1}{2}\gamma\mu_0 (n\cdot M)^2 - \frac{1}{2}\chi_a \mu_0 (n\cdot H)^2 \qquad (1)$$

Let φ be the angle between the unperturbed nematic director $\boldsymbol{n}_0$ and $\boldsymbol{n}$, and ψ the angle between $\boldsymbol{n}_0$ and $\boldsymbol{M}$. We take the magnetic field to be along $\boldsymbol{n}_0$ and neglect the last term in f. Then:

$$f = f_0 + \frac{1}{2}K\left(\frac{\mathrm{d}\varphi}{\mathrm{d}x}\right)^2 - \mu_0 MH\cos\psi - \frac{1}{2}\gamma\mu_0 M^2\cos^2(\varphi-\psi) \qquad (2)$$

There is also a gradient term $\frac{1}{2}A\left(\frac{\mathrm{d}\psi}{\mathrm{d}x}\right)^2$ due to magnetic dipolar interactions. The coefficient A is spin-wave stiffness and can be estimated[31] to be of the order of $A \approx 10^{-14}$ N, which is much smaller than the typical value of $K \approx 10^{-12}$ N, and is neglected. The addition of this term would renormalize elastic constant K in the expressions for relaxation rates. Expansion to harmonic terms for small fluctuations in φ and ψ and taking fluctuations with a given wavenumber q leads to two coupled modes with relaxation rates:

$$\frac{1}{\tau} = \frac{1}{2\eta}\left[Kq^2 + 2\gamma\mu_0 M^2 + \mu_0 HM \pm \sqrt{(Kq^2 - \mu_0 HM)^2 + 4\gamma^2\mu_0^2 M^4}\right] \qquad (3)$$

Here η is an effective viscosity. Expansion to linear terms in H gives for the slower mode:

$$\frac{1}{\tau} = \frac{1}{2\eta}\left[Kq^2 + 2\gamma\mu_0 M^2 - \sqrt{K^2q^4 + 4\gamma^2\mu_0^2 M^4} + \mu_0 HM\left(1 + \frac{Kq^2}{\sqrt{K^2q^4 + 4\gamma^2\mu_0^2 M^4}}\right)\right] \qquad (4)$$

Comparing the term independent of H and the coefficient of H with experiment, and using the known value of $K = 3.5 \times 10^{-12}$ N, we get an estimate for γ.

The threshold field B_c for the beginning of the reversal of M_s is obtained from the relaxation rate of the fundamental director mode (with $q = \pi/d$, where d is the sample thickness), which at threshold goes to 0 and leads to:

$$B_c = \mu_0 H_c = -\frac{\gamma\mu_0 M_s^2 K\pi^2}{K\pi^2 + \gamma\mu_0 M_s^2 d^2} \qquad (5)$$

31. Liechtenstein, A. I., Katsnelson, M. I. & Gubanov, V. A. Exchange interactions and spin-wave stiffness in ferromagnetic metals. *J. Phys. F* **14,** L125–L128 (1984).

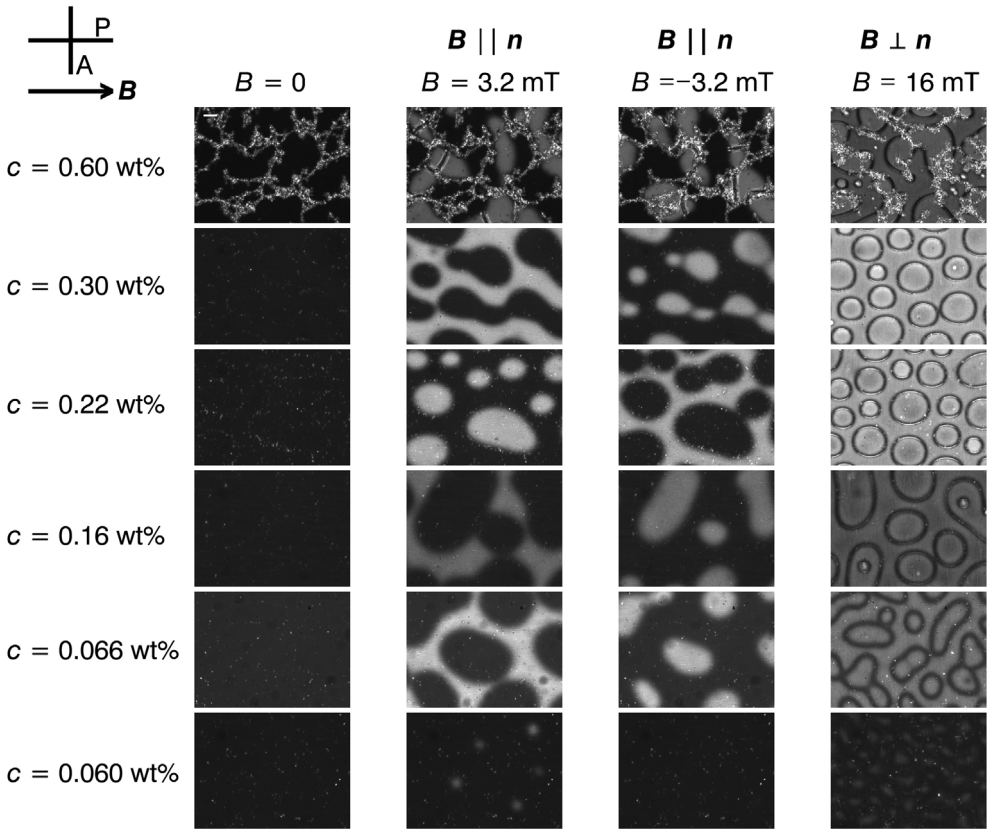

Extended Data Figure 1 | Images of polydomain samples with different concentrations of magnetic nanoplatelets in an external magnetic field. The director lies in the plane of the sample either parallel or perpendicular to the external magnetic field, *B*. P and A show directions of polarizer and analyser, respectively. The scale bar in the first image is 40 μm.

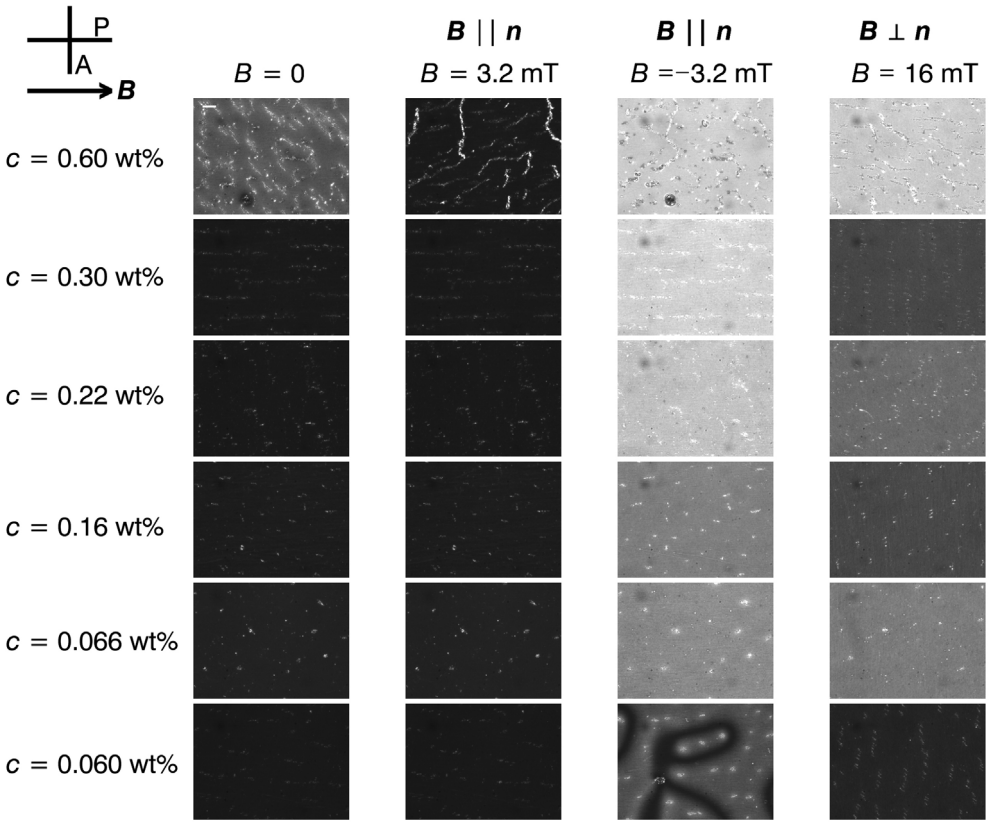

Extended Data Figure 2 | Images of monodomain samples with different concentrations of magnetic nanoplatelets in an external magnetic field. The director lies in the plane of the sample either parallel or perpendicular to the external magnetic field. The scale bar in the first image is 40 μm.

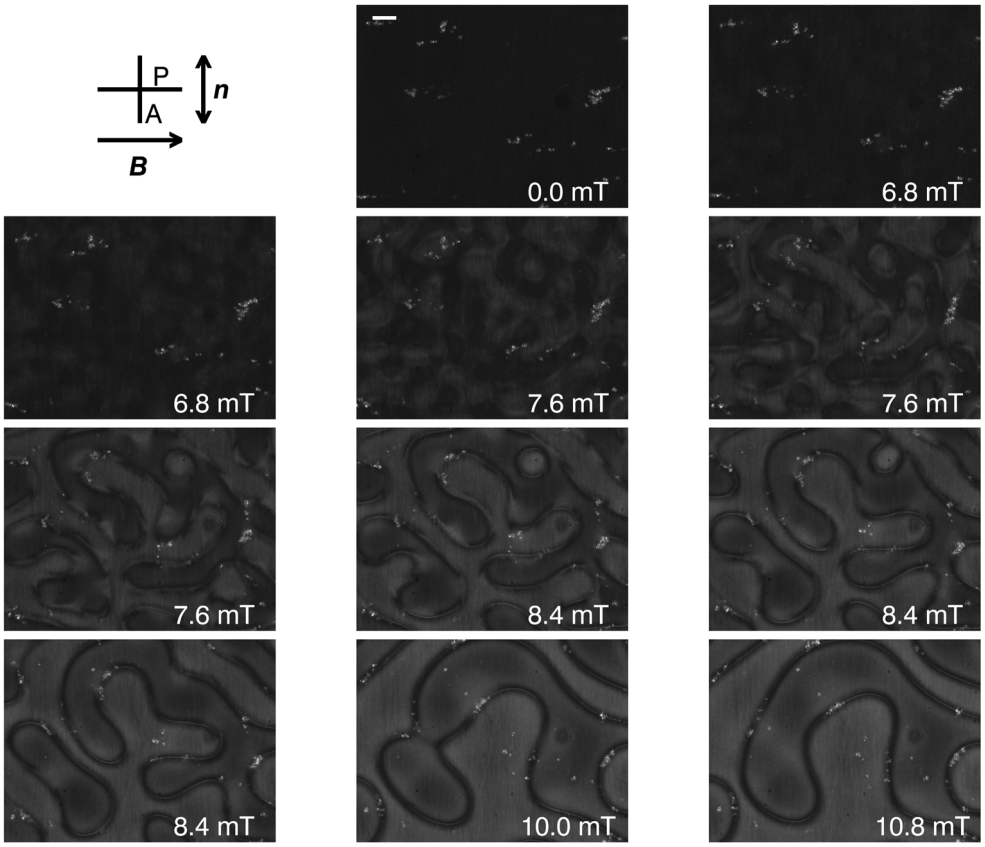

Extended Data Figure 3 | Sequence of images showing domain growth. The external magnetic field is slowly increased in a sample that was quenched in the absence of an external magnetic field. The direction of the external field is perpendicular to ***n***. If the field is switched off, the initial dark field is obtained. However, if the field is switched on immediately or within a few hours, the formed domains are still visible. The concentration of the platelets in 5CB was 0.16 wt%. The scale bar in the first image is 40 μm.

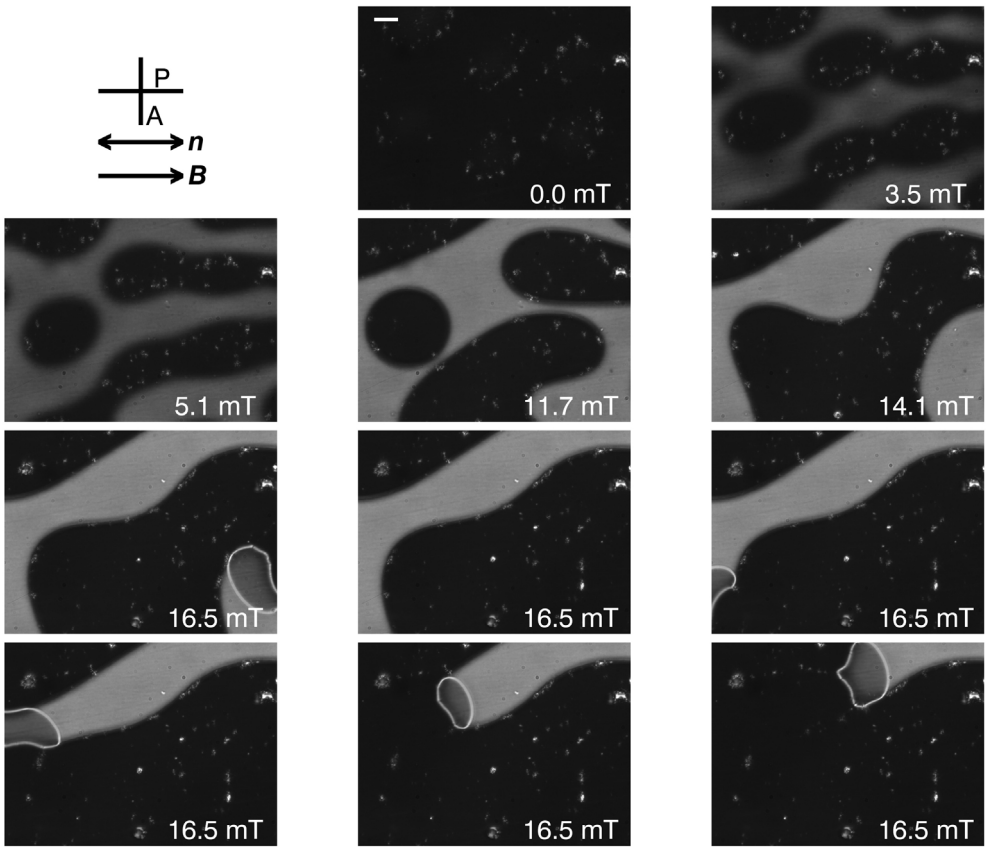

Extended Data Figure 4 | Sequence of images showing transition from a polydomain to a monodomain sample. The external field is parallel to ***n***. The white lines are the edges of domain walls. The concentration of the platelets in 5CB was 0.3 wt%. The scale bar in the first image is 40 μm.

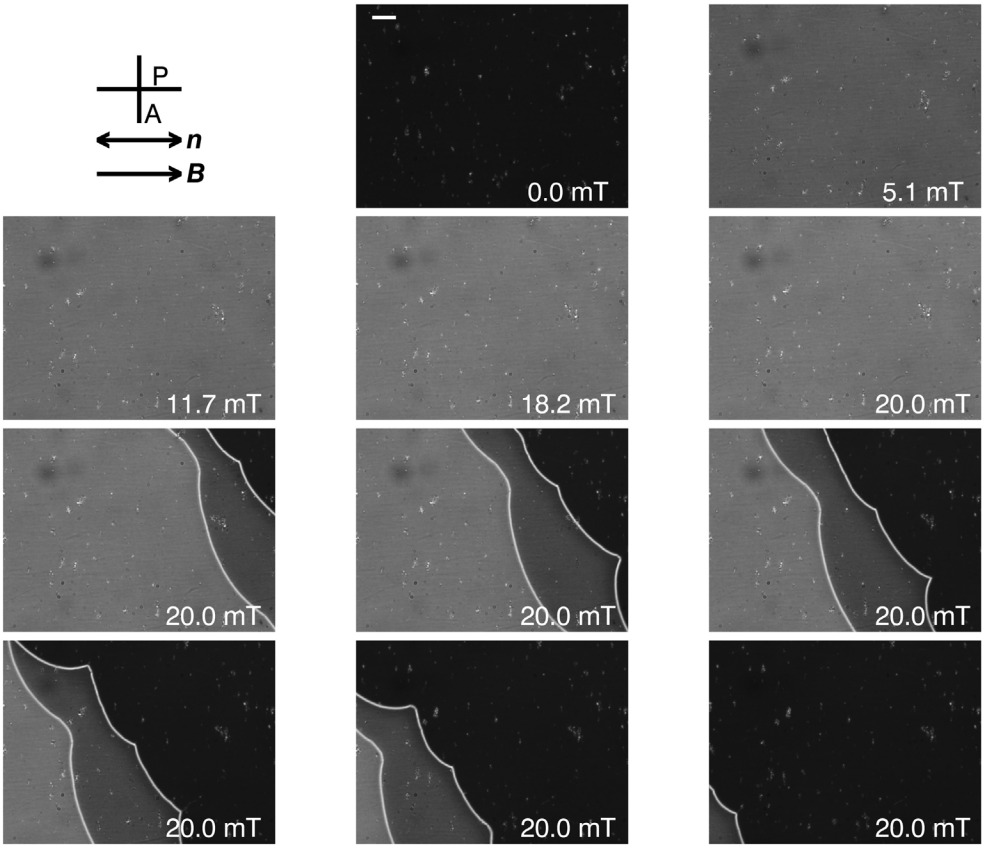

Extended Data Figure 5 | Sequence of images showing the complete switching of a monodomain sample. The field is applied parallel to ***n*** and in reverse direction to the field that was used during the quench to nematic phase and then switched off. Travelling white lines are the surface domain walls, where the director rotates by π. The concentration of the platelets in 5CB was 0.16 wt%. The scale bar in the first image is 40 μm.